# CAPTURING REYNOLDS NUMBER EFFECTS IN THE PERIODIC HILL FLOW BY USING LES WITH ANISOTROPY-RESOLVING SUB-GRID SCALE MODEL

**Matteo Montecchia, Stefan Wallin, Geert Brethouwer and Arne V. Johansson**
Department of Mechanics
KTH, Royal Institute of Technology
Osquars Backe 18, SE-10044 Stockholm, SWEDEN
matteomo@mech.kth.se

## INTRODUCTION

Wall resolved large-eddy simulation (LES) is often restricted by excessive resolution requirements and Reynolds-number scaling. A considerable reduction of computational resources is achievable by employing the Explicit Algebraic subgrid scale model (EAM) (Marstorp *et al.* (2009)).

The Explicit Algebraic subgrid scale model (EAM) has been extensively tested in wall-resolved large-eddy simulation (LES) applications and its performance has been proven by the works of Rasam *et al.* (2014) and Montecchia *et al.* (2017). The latter paper illustrates that the use of the EAM allows for a reduction of computational resources in a pseudo-spectral code. The same findings has been confirmed by using finite-volume codes, as described by Rasam *et al.* (2014). LES with EAM has been also tested with the opensource code OpenFOAM, for the channel flow geometry, by adopting a numerical technique that reduces the amount of numerical dissipation caused by the use of the Rhie & Chow interpolation. LES of periodic hill flow is carried out using OpenFOAM with the EAM and a low-diffusive implementation that has been previously tested on a turbulent channel flow at different Reynolds numbers. The aim of the present study is to evaluate in a broad sense the influence of the Reynolds number on the flow quantities in the periodic hill flow. The work of Kähler *et al.* (2016) comprises an experimental investigation of the separated flow in a channel with streamwise periodic constrictions, showing that the length of the separation bubble is reduced with increasing Reynolds number. In the same spirit, the study proposed here aims to investigate the possibility to capture this Reynolds number dependence with LES by using the novel numerical procedure in OpenFOAM with the EAM SGS model, using moderately fine resolution.

## MATHEMATICAL FORMULATION

The EAM is non-linear and derived from the modelled transport equations of SGS stress anisotropy. The expression for the modelled stress tensor reads:

$$\tau_{ij} = \frac{2}{3}\delta_{ij}K_{SGS} + \underbrace{\beta_1 K_{SGS}\widetilde{S}^*_{ij}}_{eddy-viscosity} + \underbrace{\beta_4 K_{SGS}(\widetilde{S}^*_{ik}\widetilde{\Omega}^*_{kj} - \widetilde{\Omega}^*_{ik}\widetilde{S}^*_{kj})}_{\substack{anisotropy\ of\\ SGS\ stresses}}. \tag{1}$$

where $\tau_{ij}$ is the SGS stress tensor, and $\widetilde{S}^*_{ij}$ and $\widetilde{\Omega}^*_{ij}$ are the resolved strain and rotations rate tensors, respectively, normalized by the SGS time scale $\tau^*$. $K_{SGS}$ is the SGS kinetic energy, modelled as

$$K_{SGS} = c\widetilde{\Delta}^2|\widetilde{S}_{ij}|^2, \tag{2}$$

$\widetilde{\Delta}$ is the filter scale, and the model coefficient $c$ is dynamically computed using a test filter and the Germano identity. $\beta_1$ and $\beta_4$ are model coefficients and depend on $\widetilde{S}_{ij}$ and $\widetilde{\Omega}_{ij}$. The second term on the right-hand-side of (1) is an eddy-viscosity type of term while the third non-linear term aims to improve the modelling of $\tau_{ij}$ in regions of strong anisotropy. Previous studies have proven that EAM significantly improves LES of rotating and non-rotating wall-bounded turbulent flows (Marstorp *et al.* (2009), Rasam *et al.* (2011), Rasam *et al.* (2014)). A recent study by Montecchia *et al.* (2017), where a pseudo-spectral code is employed, has shown that LES with EAM is more accurate especially at coarse resolutions, than the eddy viscosity SGS models like the dynamic Smagorinsky model (DSM). Large differences in the prediction of the Reynolds stress tensor components and the mean velocity profiles are noticeable for a range of channel flow friction Reynolds number starting from $Re_\tau \approx 550$ up to $Re_\tau \approx 5200$. The friction Reynolds number is based on the friction velocity and the channel half-width and the streamwise grid spacing is $\Delta x^+ \approx [157, 270]$, while the spanwise one is $\Delta z^+ \approx [63, 108]$ in the LES. The better performance of the EAM can be attributed to the third term on the right-hand-side of (1), which gives a significant contribution near the wall.

## RESULTS

### Turbulent Channel Flow

LES of incompressible turbulent channel flow has been performed at the friction Reynolds number of 550, by using the open-source, finite volume code OpenFOAM. A mass-flow constraint has been imposed, such that the bulk Reynolds number is the same as the DNS of Hoyas & Jiménez (2006), and the resolution used is $(\Delta x^+, \Delta z^+) \approx (41, 27)$. Two different SGS models have been employed, the Dynamic Smagorinsky Model (DSM) (Germano *et al.* (1991)) and the Explicit Algebraic SGS model (EAM). A modified version of the OpenFOAM solver `pimpleFoam` that reduces the numerical dissipation given by the Rhie and Chow (R&C) interpolation has been used (Montecchia *et al.*

(2018)). By tuning the $\beta_p$ coefficient to a value of 1, a full influence of R&C interpolation on the numerical scheme is achieved, while that can be assumed as negligible by selecting a very small value, $\beta_p = 0.01$ is the value that has been used in the following simulations. Figure 1 a) shows the streamwise component of the Reynolds stress tensor along the wall-normal direction in inner units. For the results obtained with OpenFOAM (in solid lines), the LES with EAM gets closer to the DNS reference data than the LES with DSM, especially in proximity of the inner layer peak. Similar and consistent results are achieved with the pseudo-spectral code (shown in figure 1), but with a much coarser resolution, of $(\Delta x^+, \Delta z^+) \approx (144, 58)$. The prediction of the turbulence intensity (shown in figure 1 a)) as well as the mean velocity profile is substantially improved by using $\beta_p = 0.01$ as compared to LES carried out with the R&C interpolation in the numerical scheme (*i.e.* $\beta_p = 1.0$).

The streamwise two-point correlation coefficient of the streamwise velocity, computed at $y^+ \approx 10$ is presented in figure 1 b). The green line refers to LES with the DSM, and with a full R&C interpolation. The reference DNS data is computed at $Re_\tau \approx 590$. The LES data with DSM and EAM with $\beta_p = 0.01$, are represented in blue and red. The autocorrelation is essentially independent of the choice of a specific SGS model, but is influenced by the R&C interpolation. By reducing the R&C interpolation, the autocorrelation gets much closer to the DNS. In other words, the new numerical procedure with a reduced numerical dissipation allows for a better estimation of the streamwise extension of the streaks that are generated close to the wall, independently of the SGS model used.

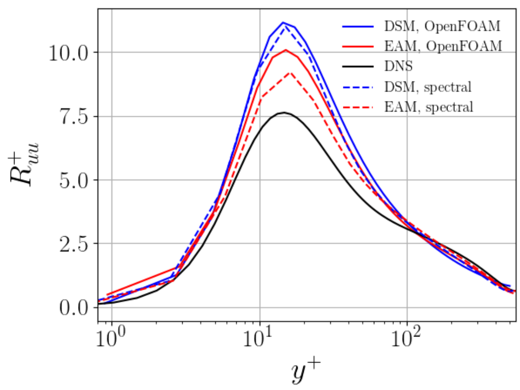


a)

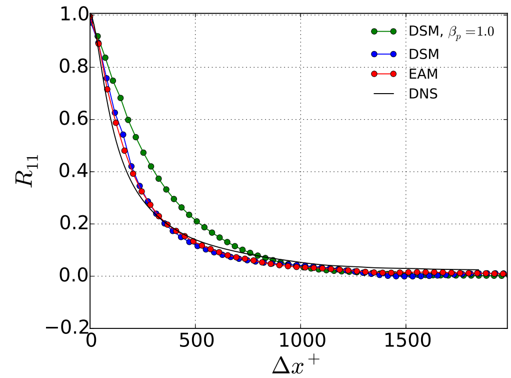


b)

Figure 1. a) Streamwise Reynolds stress as a function of the wall-normal direction in wall units. b) Two-point correlation coefficient of the fluctuating part of the streamwise Reynolds stress with a separation $\Delta x^+$, at $y^+ \approx 10$.

## Periodic Hill Flow

The behaviour of the EAM model has been extensively analyzed in simple wall-bounded flows. However, the performance of LES with EAM with OpenFOAM in more complex geometries is still an open question. As pointed out in Montecchia *et al.* (2018), it is not clear yet if the new numerical scheme approach can be applied to such configurations without side-effects. By using the same R&C interpolation-free numerical scheme, the second part of the study consists of an LES of a periodic hill channel flow with a Reynolds number based on the bulk velocity at the hill top and hill height of $Re_h = 10595$. The streamwise, wall-normal and spanwise dimensions are $L_x = 9.0h$, $L_y = 3.035h$, $L_z = 4.5h$, respectively, where $h$ is the height of the hill. A backward discretisation scheme in time has been adopted, together with a second-order space discretisation. For numerical stability reasons, the CFL number has been kept to 0.1. The simulations are run over a time horizon of $20t_x$, where $t_x = L_x/u_b$ is the flow-through time and $u_b$ the bulk velocity, then the statistics are collected over a period of $140t_x$.

A coarse and a fine mesh have been adopted. The coarse mesh (denoted as "C") has the following discretisation, $N_{xyz} = 100 \times 120 \times 70$, while the fine mesh (denoted as "F") has less than 2 million grid points, distributed as $N_{xyz} = 148 \times 156 \times 92$. Note that the mesh F is about 6 times coarser than the reference LES, from the work of Breuer *et al.* (2009), which employs a mesh with about 13 million grid points. The mesh geometry, very similar for all the cases, presents a clustering of the grid near the upper and lower walls to better resolve the attached boundary layers, with a first-cell thickness constraint of $y^+ \approx 1$ . An additional refinement in the streamwise direction is done so the grid spacing is halved in proximity of the periodic constrictions.

In figure 2 the resolutions in wall units in all the directions are shown. As we can see, the grid is designed so that the inner-scaled wall-normal discretisation is fairly constant in the streamwise direction. The stream- and spanwise resolutions, are instead reduced when the number of grid points gets larger, passing from the streamwise-averaged values of $(\Delta x^+, \Delta z^+) \approx (27, 20)$ to $(\Delta x^+, \Delta z^+) \approx (20, 17)$.

LES are carried out with the DSM and the EAM. Furthermore, an additional case (denoted with "EAMRC") has been performed by using the EAM and the standard OpenFOAM solver with full R&C interpolation and therefore $\beta_p = 1.0$.

**Friction coefficient** The positions in the streamwise direction of the flow separation and reattachment by using the zero friction coefficient criterion are given in table 1. The sensitivity of the different SGS models to the flow dramatically decreases when the coarse mesh C is adopted, especially on the estimation of the separation point but also unsatifactory results are obtained for the reattachment point. On the other hand, the increase of resolution given by the mesh F leads to a distinction of the prediction of the positions for the different SGS models.

The friction coefficient along the streamwise direction is shown in figure 3. The skin friction peak due to a flow acceleration ($x/h \approx 9$), is underestimated for all the models. However, LES with EAM gives a slightly better estimation

Table 1. Summary of the periodic hill simulations, $Re_b = 10595$.

| Case | $N_x \times N_y \times N_z$ | $(\frac{x}{h})_{sep}$ | $(\frac{x}{h})_{reat}$ |
|---|---|---|---|
| EAM-C | $100 \times 120 \times 70$ | 0.24 | 5.40 |
| EAMRC-C | $100 \times 120 \times 70$ | 0.20 | 5.45 |
| DSM-C | $100 \times 120 \times 70$ | 0.24 | 4.28 |
| EAM-F | $148 \times 156 \times 92$ | 0.24 | 4.68 |
| EAMRC-F | $148 \times 156 \times 92$ | 0.20 | 4.72 |
| DSM-F | $148 \times 156 \times 92$ | 0.24 | 4.36 |
| REFLES | $280 \times 220 \times 200$ | 0.19 | 4.69 |

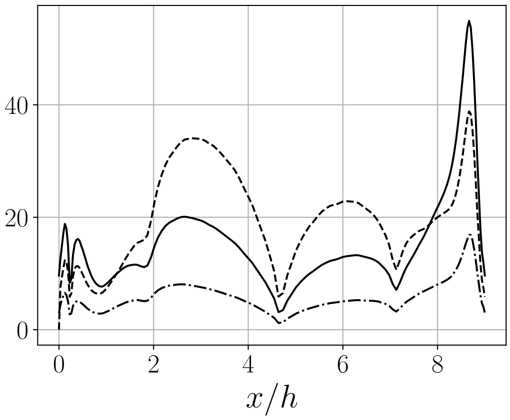


Figure 2. Streamwise, wall-normal and spanwise resolutions in wall units, for the mesh F. $--$ : $\Delta x^+$, $-.-$ : $10\Delta y^+$, $-$ : $\Delta z^+$

of the separation bubble, getting closer to the reference LES results. The largest deviations from the reference values are found in the region $x/h \in [4,7]$, for the DSM.

The introduction of a full R&C interpolation leads to an underestimation of the friction coefficient near the channel inlet, but similar results to LES with EAM are achieved in proximity of the separation bubble.

**Mean velocity profiles** In figure 4 streamlines of the mean flow are plotted on top of a contour plot of the instantaneous streamwise velocity, computed from the LES with EAM. There the streamwise and wall-normal positions of the recirculation bubble core are very close to the reference LES ($[x/h, y/h] \approx [2.0, 0.5]$), together with a reasonable estimation of the bubble extension.

The number of grid points in grid C is clearly not sufficient to give significant differences between SGS models in the mean flow properties, but substantial improvements can be seen when using the F mesh. The use of the EAM and the mesh F leads to a better estimation of the streamwise mean velocity profiles, shown in figure 5 as a function of the wall-normal coordinate and at different streamwise positions. The peak close to the lower wall is very well-captured at the position close to the inlet (see figure 5 a)) for the EAM, whereas LES with DSM overpredicts the peak amplitude. In contrast, small differences are noticeable close to the upper wall at the streamwise positions after the hill: a slight underpredition at $x/h = 4.0$ is found when using the EAM, and an overprediction with the LES with DSM. Large improvements, given by LES with EAM are also visible in a global sense on all the profiles, in proximity of the upper wall, there the EAM helps to improve the estimation of the inner layer peak and its results are the closest to the reference data. Increasing the amount of *R&C* interpolation together with the EAM, resulted in a deterioration of the results (especially when adopting a full *R&C* interpolation), in terms of a more accentuated misprediction in both the lower and upper wall peaks.

**Reynolds shear stresses** The prediction of the Reynolds shear stress is rather insensitive to the choice of the SGS model, over a large part of the streamwise direction. However, the computation of the shear layer dynamics is weakly sensitive to the SGS modelling. In figure 6 the Reynolds shear stress profiles are shown as a function of the wall-normal coordinate in three different positions, in proximity of the separation bubble. Even though small differences are visible between the LES with EAM and DSM, remarkable improvements occur when the diffusion driven by the R&C interpolation is reduced. A larger overestimation of the peak close to the lower wall has been experienced with the use of the standard solver (look at figures 6 a) and c)).

## CONCLUSIONS

The use of EAM, together with the new low-dissipative solver, leads to a reasonable estimation of the channel flow quantities, especially towards the wall. No side-effects due to the reduction of the R&C interpolation have been experienced in all the simulations. A moderately fine resolution of the grid, together with the use of the EAM and the low-dissipative solver, gives promising results in the periodic hill flow at $Re_b = 10595$, thus paving the way to an investigation on the flow quantities at different Reynolds numbers. However, the stability requirements of OpenFOAM for periodic hill LES are quite restricted to a rather low CFL value and the use of additional deferred correction in the velocity divergence scheme is essential for complex geometries to avoid numerical instabilities. For the present Reynolds number the choice of a proper SGS model has a much smaller influence than the choice of a proper numerical scheme and the reduction of the dissipation given by the R&C interpolation. The second part of the study, which will be shown in the presentation, will consist of the assessment of the periodic hill flow at the bulk Reynolds number $Re_b = 37000$. The wall-resolved LES for that case has been computed with a mesh of about 14 million grid points. We experienced that by increasing the Reynolds number the influence of the SGS model used gets more crucial and much larger differences are visible not only in the mean flow properties and the skin friction, but also in the Reynolds stresses.

## REFERENCES

Breuer, M, Peller, N, Rapp, Ch & Manhart, M 2009 Flow over periodic hills–numerical and experimental study in a wide range of reynolds numbers. *Comput. Fluids* **38** (2), 433–457.

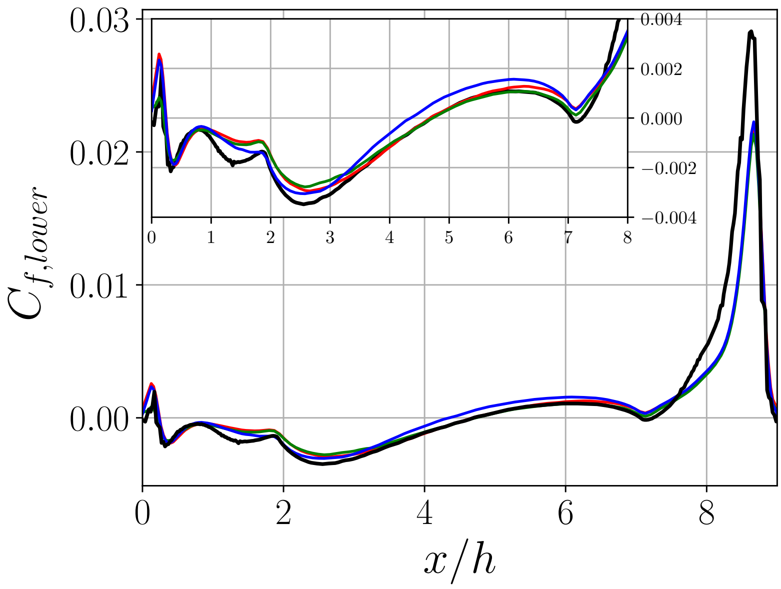


Figure 3. Skin friction coefficient at the lower wall as a function of the streamwise direction. — : DSM, — : EAM, — : EAMRC, — : reference LES.

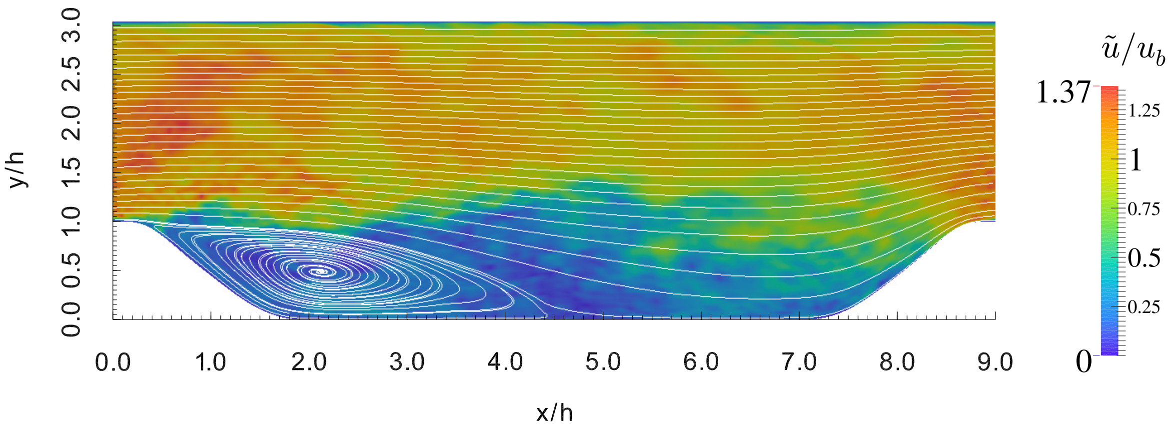


Figure 4. Streamlines of the mean flow with contourplots of the instantaneous velocity $\tilde{u}/u_b$, LES with EAM.

Germano, Massimo, Piomelli, Ugo, Moin, Parviz & Cabot, William H 1991 A dynamic subgrid-scale eddy viscosity model. *Phys. Fluids A: Fluid Dynamics (1989-1993)* **3** (7), 1760–1765.

Hoyas, Sergio & Jiménez, Javier 2006 Scaling of the velocity fluctuations in turbulent channels up to $Re_\tau = 2003$. *Phys. Fluids (1994-present)* **18** (1), 011702.

Kähler, Christian J, Scharnowski, Sven & Cierpka, Christian 2016 Highly resolved experimental results of the separated flow in a channel with streamwise periodic constrictions. *J. Fluid Mech.* **796**, 257–284.

Marstorp, Linus, Brethouwer, Geert, Grundestam, Olof & Johansson, Arne V 2009 Explicit algebraic subgrid stress models with application to rotating channel flow. *J. Fluid Mech.* **639**, 403–432.

Montecchia, Matteo, Brethouwer, Geert, Johansson, Arne V & Wallin, Stefan 2017 Taking large-eddy simulation of wall-bounded flows to higher Reynolds numbers by use of anisotropy-resolving subgrid models. *Phys. Rev. Fluids* **2** (3), 034601.

Montecchia, Matteo, Knacke, Thilo, Brethouwer, Geert, Wallin, Stefan & Johansson, Arne V. 2018 Improved LES of turbulent channel flow by using OpenFOAM with the Explicit Algebraic SGS model. *12th International ERCOFTAC Symposium on Engineering Turbulence Modelling and Measurements* .

Rasam, Amin, Brethouwer, Geert, Schlatter, Philipp, Li, Qiang & Johansson, Arne V 2011 Effects of modelling, resolution and anisotropy of subgrid-scales on large eddy simulations of channel flow. *J. Turbul.* **12**, 1–20.

Rasam, Amin, Wallin, Stefan, Brethouwer, Geert & Johansson, Arne V 2014 Large eddy simulation of channel flow with and without periodic constrictions using the explicit algebraic subgrid-scale model. *J. Turbul.* **15** (11), 752–775.

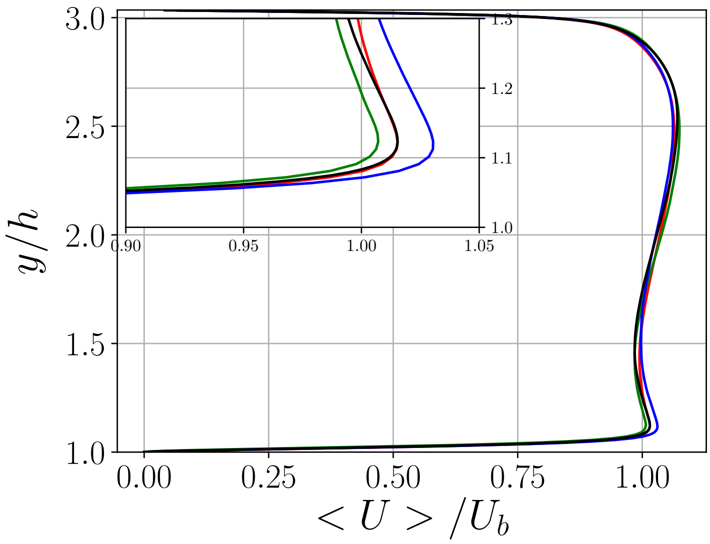


a)

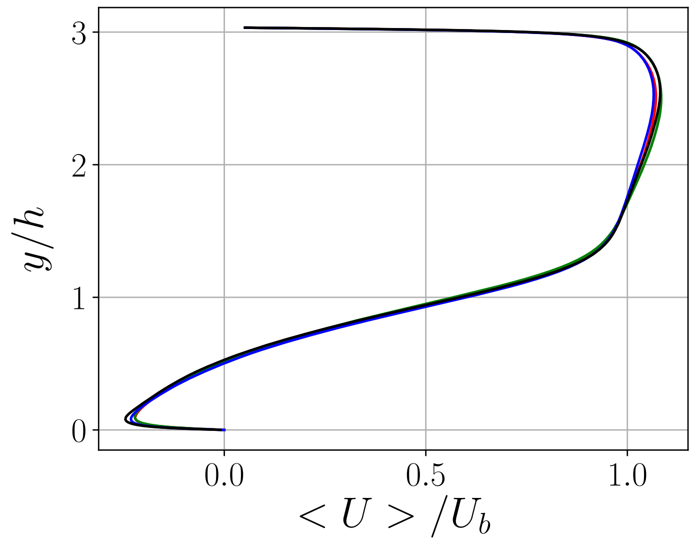


b)

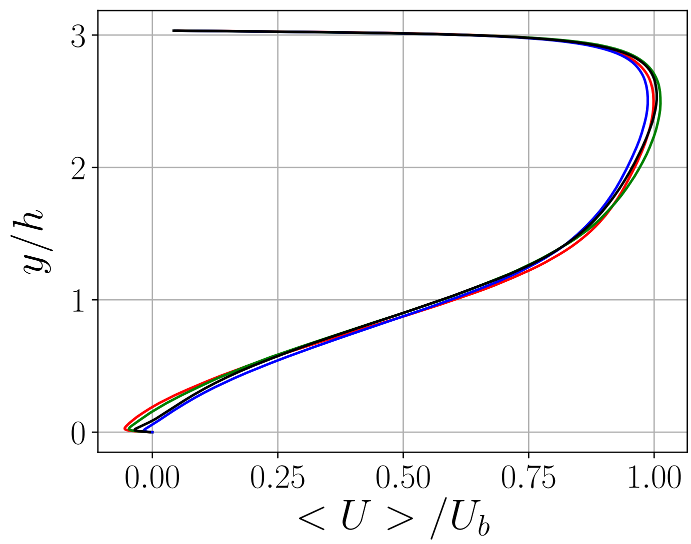


c)

Figure 5. Mean streamwise velocity profiles along the wall-normal direction at a) $x/h = 0.05$, b) $x/h = 2.0$ and c) $x/h = 4.0$.
— : DSM, — : EAM, — : EAMRC, — : reference LES,

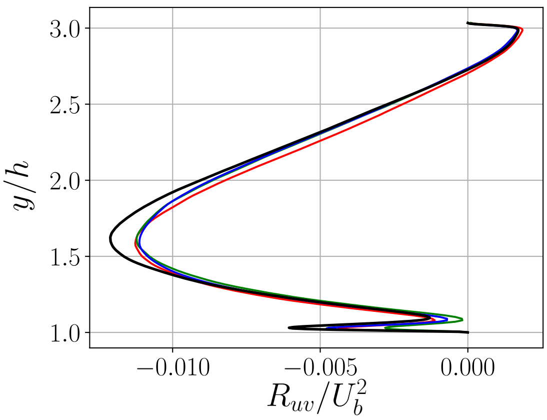


a)

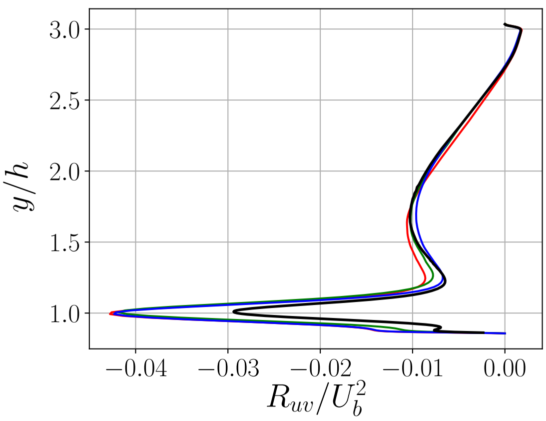


b)

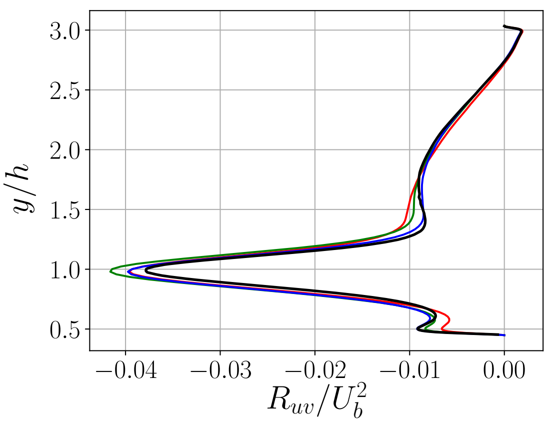


c)

Figure 6. Reynolds shear stress along the wall-normal direction at a) $x/h = 0.05$, b) $x/h = 0.5$ and c) $x/h = 1.0$. — : DSM, — : EAM, — : EAMRC, — : reference LES,